Desalination and Water Treatment
www.deswater.com

doi:10.5004/dwt.2018.22747

120 (2018) 261–271
July

Kinetics and equilibrium study for the adsorption of lysine on activated carbon derived from coconut shell

Jinbei Yang[a,*], Shuicui Han[b]

[a]*School of Ocean Science and Biochemistry Engineering, Fuqing Branch of Fujian Normal University, Fuzhou 350300, Fujian, China, Tel. +86-15280192415, email: yangjinbei@sina.com (J. Yang)*
[b]*Department of Chemical Engineering, Zhicheng College of Fuzhou University, Fuzhou 350002, Fujian, China, Tel. +86-13960885921, email: hanshucui@163.com(S. Han)*

Received 13 December 2017; Accepted 5 July 2018

ABSTRACT

Activated carbon was prepared from coconut shell by a chemical activation method with potassium hydroxide at different temperatures and characterized for pore structure. The adsorption of lysine from aqueous solution by the prepared coconut shell activated carbon was carried out using batch adsorption experiments. The effect of shaking speed, adsorbent dosage, pH, initial lysine concentration and temperature were investigated. The results indicate that coconut shell activated carbon is an effective adsorbent which has a high surface area (1118.2 m^2/g) and pore volume (0.4992 cm^3/g). The effect of external diffusion is negligible at 170 rpm, the percent removal of lysine increases with the increment of the adsorbent dosage, the optimum pH is 6. The adsorption equilibrium data obtained at 20, 30 and 40°C agree better with the Langmuir model than with Freundlich model, and the thermodynamics parameters, ΔH = 2.71 kJ/mol, ΔS = 107.2 J/mol·K and $\Delta G < 0$, display that the adsorption process is spontaneous and endothermic. The adsorption kinetics is well described by the pseudo second-order equation. The activated carbon was successfully regenerated by using ammonia as eluent. The results exhibit that coconut shell activated carbon is an efficient and low-cost adsorbent for the removal of lysine from aqueous solutions.

Keywords: Lysine removal; Adsorption; Isotherm; Kinetics; Coconut shell

1. Introduction

Lysine is one of the essential amino acids in human body [1,2]. It can promote the development of human body, enhance the immune function and improve the function of the central nervous system [3–5]. The content of lysine in cereal food is very low and it is easy to be destroyed in food processing [6,7]. Therefore, it is called the first limiting amino acid and used as food fortifier and feed additive. There are many methods to synthesize lysine, such as microbial fermentation, enzymatic and chemical synthesis [8,9]. Among them, microbial fermentation is the main mode of production. Twenty-three hundred thousand tons of lysine are annually produced worldwide by microbial fermentation, and the production is steadily increasing year by year.

In the process of fermentation, a large amount of wastewater containing lysine is produced [10]. There are many methods for the treatment of amino acid-containing effluents including aerobic and anaerobic biological treatments [11], electrodialysis [12,13], precipitation [14], membrane filtration [15,16], and adsorption [17,18]. The first four methods are efficient but they have many disadvantages, such as the high required energy, the production of solid waste, and causing secondary pollution. Among them, adsorption is the most commonly used method for water and wastewater treatment because of its simple operation, high efficiency and low cost [19]. A number of adsorbents have been reported for the removal of amino acids, such as mesoporous silica [20,21], moroccan diatomite [22], milk thistle seeds [23], polymeric adsorbent [24], activated carbon [25], etc. Activated carbon is regarded as one of the most

*Corresponding author.

effective and usual adsorbent due to its high surface area, pore volume and excellent efficiency. Therefore, it is one of the most significant adsorbents for the removal of amino acids from wastewater. Nevertheless, due to its relatively high cost, growing research interest is focused on finding the naturally available and cheap alternatives to replace commercial activated carbons [26,27]. The development of high efficiency and low-cost activated carbon is beneficial to environmental sustainability and commercial applications in the future. Biomass materials mainly derived from agricultural wastes are superior precursors for activated carbon, which are renewable, cheaper and abundantly available. There are many biomass materials having been successfully used to produce activated carbon in recent years, such as tea leaf [28], date palm rachis and jujube stones [29], sewage sludge [30], the residue of desilicated rice husk [31], walnut shell [32], brewer's spent grains [33], grape bagasse [34], coffee residues and almond shells [35], hazelnut shell [36], Acacia fumosa seed [37], coconut shell [38,39], etc. As a typical biomass, coconut shell is widely available and a suitable precursor to prepare activated carbon [40,41].

The purpose of this paper is to study the adsorption of lysine from aqueous solution by the activated carbon prepared from coconut shell. The effects of shaking speed, adsorbent dosage, pH, initial lysine concentration and temperature on the static adsorption of lysine onto the prepared activated carbon were investigated by batch experiments. Moreover, the adsorption isotherms and kinetics of lysine on coconut shell activated carbon at different temperatures were also studied.

2. Experimental

2.1. Materials

Potassium hydroxide, ninhydrin and sodium acetate (analytical grade) were supplied by Sinopharm Chemical Reagent Co., Ltd, glacial acetic acid (analytical grade) were supplied by Shanghai Qiangshun Chemical Reagent Co., Ltd, lysine（BR）were supplied by Shanghai Kangda Amino Acid Factory. Coconut shells were obtained from Hainan Province.

2.2. Analysis method

The lysine concentrations were determined by a visible spectrophotometer (model 7200, Shanghai Unico Instrument Co., Ltd) at 570 nm. The standard curve of lysine concentration (y, mg/L) to absorbance (x) is obtained as follows: $y = 18.432x + 3.8195$, the scope of x is 0–1.1, and the correlation coefficients is 0.999.

2.3. Activated carbon preparation and characterization

The coconut shells were adequately cleaned in distilled water and dried at 110°C. After that, they were crushed by a high-speed multifunction grinder (model DS-T250, Shanghai Dingshuai Instrument Co., Ltd) and separated using sieves and shakers to the size of 100 mesh. The coconut shell powder was carbonized at 300–400°C in a box-type resistance furnace (model SX2-4-10, Shanghai Experiment Instrument Co., Ltd). Then the char produced from the carbonization process was mixed with potassium hydroxide (KOH). The dried mixture was then activated under 600–800°C. After cooling, they were washed with distilled water to neutral, and dried to be activated carbon. Then, the coconut shells activated carbon was stored in desiccator for use in adsorption studies.

An orthogonal experimental design L9(3^4) was utilized in the preparation of coconut shells activated carbon as listed in Table 1. The mass ratio of carbonized material to KOH, activation time, activation temperature and carbonization temperature were set as the four influence factors, and three levels were chosen for each factor. The equilibrium adsorption capacity of lysine on coconut shells activated carbon were chosen as the investigation target to qualitatively analyze the effects of the selected factors on the preparation of coconut shells activated carbon.

The morphology and structure of the adsorbents were characterized via a Nova NanoSEM 230 scanning electron microscopy (SEM, USA FEI Co., Ltd.). A thermal gravimetric analysis was measured using a Netzsch STA449C instrument (Netzsch Co., Ltd., Gemerny). The BET specific surface area and pore size was carried out on a Micromeritics ASAP2020 equipment (Micromeritics Instrument Co., Ltd., American).

2.4. Batch adsorption of lysine on coconut shell activated carbon

2.4.1. Effect of shaking speed

0.05 g of coconut shell activated carbon was added to a 100 mL conical flask with 25 mL of 400 mg/L lysine solution. The flask was sealed and shaken on an air bath constant temperature oscillator (model THZ-C, Taicang Huamei Instrument Co., Ltd.) in the shaking speed value range 70–220 rpm, and the temperature was fixed at 30°C. Samples were analyzed as described (Section 2.2) and the adsorption capacity of lysine per unit mass of adsorbent, q_t (mg/g), was calculated by the following equation:

$$q_t = \sum_{i=1}^{n} \left(C_{i-1} - C_i\right) \times \frac{V_i}{m} \tag{1}$$

Table 1
Orthogonal experimental design L9(3^4) on the preparation of coconut shells activated carbon

Factor levels	A (carbonized material/KOH ratio)	B (activation time/h)	C (activation temperature/°C)	D (carbonization temperature/°C)
1	1	0.5	600	300
2	2	1.0	700	350
3	4	1.5	800	400

where C_i and C_{i-1} are the concentrations of lysine in the aqueous phase before and after adsorption, respectively (mg/L), V_i is the volume of the solution (L), m is the mass of adsorbent (g), and n is the sampling number. The curves between q_t and time t were plotted to acquire the adsorption rate curve at different shaking speeds.

2.4.2. Effect of adsorbent dosage

Various dosages (from 0.003–0.08 g) of coconut shell activated carbon was mixed with 25 mL of 400 mg/L lysine solutions. The solutions were shaken at 170 rpm and 30°C for 5 h. Samples were analyzed and the percent removal of lysine, R, was calculated according to Eq. (2).

$$R = \frac{(C_0 - C_e)}{C_0} \tag{2}$$

where C_0 and C_e (mg/L) are the concentrations of lysine at initial and equilibrium in the solution, respectively.

2.4.3. Effect of pH value

Coconut shell activated carbon, 0.1 g, was placed into a series of flasks with 25 mL of lysine solution (400 mg/L). The pH (from 1 to 7) of solutions were obtained using 0.1 M H_2SO_4. The flasks were then sealed and shaken at 170 rpm and 30°C for 5 h to ensure equilibrium. Samples were taken and analyzed, respectively. The equilibrium adsorption capacity of lysine, q_e (mg/g), was calculated using Eq. (3):

$$q_e = \left[\frac{(C_0 - C_e)}{m}\right] \times V \tag{3}$$

where V is the volume of the solution (L).

2.4.4. Adsorption isotherm

The coconut shell activated carbon, 0.05 g and 25 mL of lysine solution with different initial concentrations (100, 200, 300, 400, 500, 600, and 700 mg/L) were placed into each conical flask. The solutions were shaken at 170 rpm for 5 h under the temperature of 20, 30 and 40°C, respectively. The samples were taken and analyzed by visible spectrophotometer as described in section 2.2. Each equilibrium concentration of lysine was obtained, and the corresponding equilibrium adsorption capacity was determined. Thus, the adsorption equilibrium curves at 20, 30 and 40°C were obtained by plotting the data of q_e vs. C_e, respectively.

2.4.5. Adsorption kinetics

The adsorption kinetic experiments were performed as follows: The coconut shell activated carbon, 0.05 g, and 25 mL of lysine solution with initial concentrations 400 mg/L was put into conical flask. The shaking speed was fixed at 170 rpm, the temperature was 20, 30 and 40°C, respectively. The samples were taken and analyzed at approximately intervals, and the adsorption capacity of lysine was calculated according to Eq. (1). The data between q_t and time t were obtained under the different temperatures. Furthermore, the pseudo first order and pseudo second-order kinetic models were used to correlate the kinetic of the adsorption data in order to obtain the controlling mechanism of the adsorption processes.

2.5. Desorption study

The lysine recovery experiments was employed by using different concentrations of ammonia as eluent. After lysine adsorption, the activated carbon loaded with lysine was air-dried. Then, 0.05 g of the activated carbon loaded with lysine was placed in flask with 25 mL eluent solution and shaken at 170 rpm for 4 h at 30°C. The sample was taken, and the lysine concentration was determined.

3. Results and discussion

3.1. Adsorption orthogonal experiments of lysine on activated carbon

The equilibrium adsorption capacities of lysine on coconut shell activated carbon prepared at various conditions are shown in Table 2. Through the range analysis, the order of influence factors is: activation temperature, activation time, carbonization temperature, and carbonized material/KOH ratio [42,43].

The orthogonal experiment results indicate that the largest adsorption capacity of lysine on coconut shell activated carbon is found at treatment 6, which was prepared under the following conditions: carbonized material/KOH ratio of 2.0, activation time of 1.5 h, carbonization temperature of 600°C and activation temperature of 350°C, respectively. The activated carbon prepared under these conditions was used for subsequent adsorption experiments.

3.2. Characterization of the activated carbon

3.2.1. SEM

The SEM images of the precursor and the activated carbon samples is illustrated in Fig. 1, which vividly demonstrates the alteration of the physical structure. Coconut shell material surface displayed in Fig. 1a is smooth and less porosity. Fig. 1b shows the surface pores

Table 2
Experiment conditions and adsorption capacity of lysine on coconut shell activated carbon

No.	A	B/ h	C	D	q_e/(mg·g^{-1})
1	1	0.5	600	300	165.13
2	1	1.0	700	350	169.79
3	1	1.5	800	400	154.94
4	2	0.5	700	400	167.73
5	2	1.0	800	300	143.42
6	2	1.5	600	350	177.81
7	4	0.5	800	350	147.16
8	4	1.0	600	400	166.47
9	4	1.5	700	300	171.03

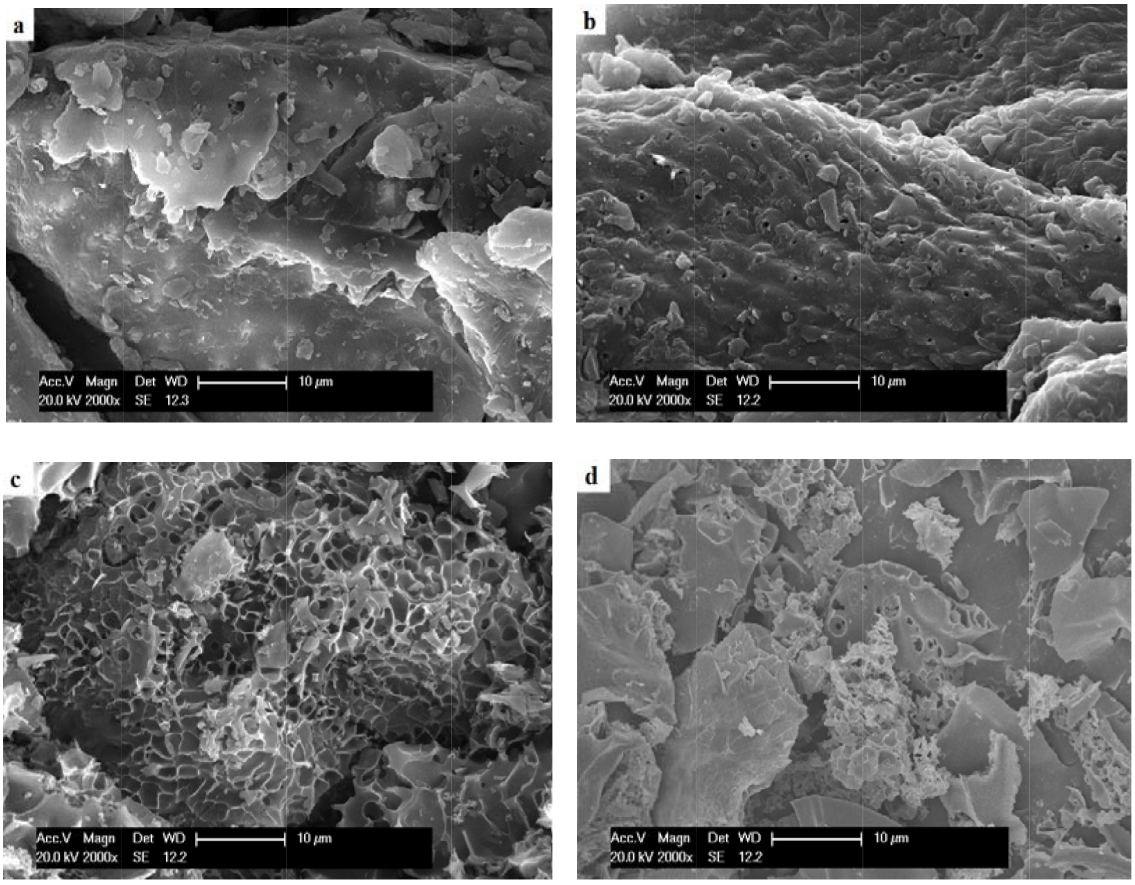

Fig. 1. SEM images of (a) raw coconut shell, (b) coconut shell after carbonization, (c) coconut shell activated carbon by chemical activation with KOH, and (d) coconut shell activated carbon after adsorption.

increased after carbonization, which is due to the release of volatile compounds during the carbonization process. It is evident that the carbon treated by potassium hydroxide has a much higher degree of pore development than that of carbonization process as can be seen from Fig. 1c, the result indicates that coconut shell activated carbon is an effective adsorbent which has the maximum surface area and pore volume compare to the raw coconut shell and carbonized material. Fig. 1d exhibits the surface pores of coconut shell activated carbon decrease after adsorption, which is mainly due to the pore channel occupied by the adsorbed lysine.

3.2.2. Nitrogen adsorption-desorption

Furthermore, the adsorption and desorption isotherms of N_2 and the pore size distribution of the precursor and the activated carbon samples are shown in Figs. 2 and 3, respectively. The data of adsorption isotherms of N_2 were acquired over a wide relative pressure range (0–0.9981). The micropore area and external surface area of coconut shell activated carbon were calculated using T-plot method. The surface area was calculated by BET equation in the range of relative pressure from 0.006 to 0.10. The micro pore volume and size distribution were determined by the Horvath-Kawazoe method. The total pore volume was obtained by the amount of N_2 adsorbed. The value

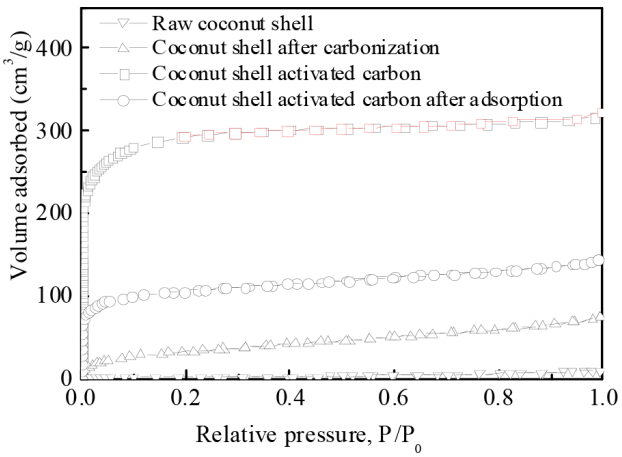

Fig. 2. N_2 adsorption and desorption isotherm of the precursor and the activated carbon samples.

of meso pore volume is the total pore volume minus the micro pore volume.

As seen from Fig. 2, the N_2 adsorption capacity of raw coconut shell was very small, indicating fewer pores. After carbonization, the coconut shell has a higher specific surface area and larger pore volume due to the removal of ash.

After chemical modification by KOH, the prepared coconut shell activated carbon yields a type I isotherm and with an important adsorption at low relative pressure, indicative of the presence of micro pore. The physical properties of the precursor and the activated carbon samples are exhibited in Table 3. The surface area, total pore volume, and average pore diameter of coconut shell activated carbon are 1118.2 m^2/g, 0.4992 cm^3/g and 0.49 nm, respectively, which display its excellent adsorption property when compared to the other two precursors. As exhibited in Fig. 3 and Table 3, micro pore volume of coconut shell activated carbon makes up 89% of total pore volume, which is much larger than meso pore volume. As reported in [44], the smaller the particle size of a porous carbon, the higher rate of the diffusion and adsorption. The results further demonstrate that the prepared coconut shell activated carbon is an outstanding adsorbent for lysine. It can also be seen from Table 3 that there are a sharp decline in the surface area, total pore volume, and average pore diameter of coconut shell activated carbon after adsorption. This phenomenon has also been observed by SEM.

3.2.3. TG-DTG

Coconut shells consist mainly of hemicellulose, cellulose and lignin, and the decomposition of hemicellulose, cellulose and lignin occurred at ranges of 180–240, 230–310, and 300–400°C, respectively [45]. The TG-DTG analysis was carried out to study the thermal stability of the precursor and the activated carbon samples, as shown in Fig. 4. As can be seen in Fig. 4a, the pyrolysis of raw coconut shells included four periods: an initial weight loss of 2.4% below 104°C is attributed to the removal of hygroscopic water. The dramatic weight loss occurs at 152–405°C with the sharp three DTG peaks at 198, 260 and 315°C corresponding to the decomposition of hemicellulose, cellulose and lignin, respectively. It resulted in a carbon residue of 43.2% at 405°C. As the temperature increases over 405°C, the weight loss becomes slowly. The carbon residue decreases to 36.5% at 600°C and 35.7% at 700°C. The decomposition of coconut shell after carbonization takes place in two stages, shown in Fig. 4b. The first stage that obtained at 35–152°C indicates the loss of adsorbed water is 2.6%. In the second stage, sharp weight loss of the raw material was 63.5% at 152–600°C in which mainly lignin fractions decompose. Figs. 4c and d show the results from TGA carried out on coconut shell activated carbon before and after adsorption. Both of the DTA curves show an endothermic peak at 68°C due to the dehydration process. Both of the TG curves demonstrate that the prepared coconut shell activated carbon has good thermal stability.

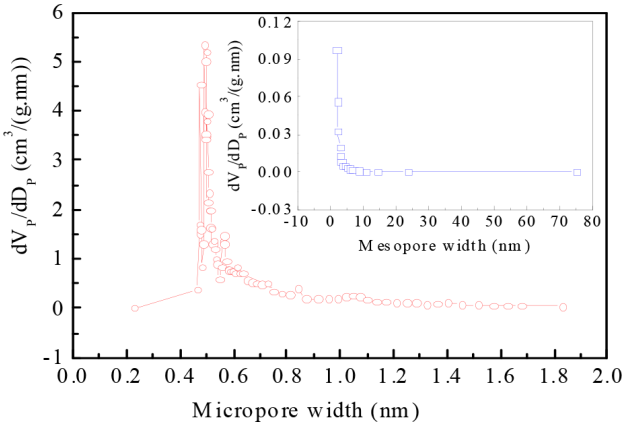

Fig. 3. Micro pore size distribution of coconut shell activated carbon. (Inset curve: the mesopore size distribution).

3.3. Adsorption studies

3.3.1. Effect of shaking speed

The adsorption rate curves (q_t vs. t) at different shaking speeds were plotted and exhibited at Fig. 5a. As shown in the figure, the adsorption rate increases with an increase in shaking speed from 70 to 170 rpm and then basically remain unchanged, which exhibits that the effect of external diffusion can be negligible. Therefore, the shaking speed of 170 rpm was selected for further studies.

3.3.2. Effect of adsorbent dosage

The effect of adsorbent dosage is depicted in Fig. 5b, which exhibits the removal of lysine as a function of adsorbent dosage. It is clearly evident that an initial increase the adsorbent dosage increases the percent removal of lysine due to the increased active sites for adsorption. Nevertheless, beyond a dosage of 0.05 g, the fractional removal appeared to be consistently close to 81.0%. The results also

Table 3
BET surface properties of activated carbon

Parameters	Raw coconut shell	Coconut shell after carbonized	Coconut shell activated carbon	Coconut shell activated carbon after adsorption
BET Surface area, S_{BET} (m^2/g)	4.2	120.7	1118.2	378.9
Micropore area, S_{micro} (m^2/g)	–	22.7	876.5	292.3
External surface area, S_{ext} (m^2/g)	11.9	97.9	241.7	86.5
Micropore volume, V_{micro} (cm^3/g)	0.0015	0.0437	0.4446	0.1569
Mesopore volume, V_{meso} (cm^3/g)	0.0134	0.0701	0.0546	0.1569
Total pore volume, V_T (cm^3/g)	0.0149	0.1138	0.4992	0.2223
Average pore diameter, APD (nm)	1.09	1.12	0.49	0.53

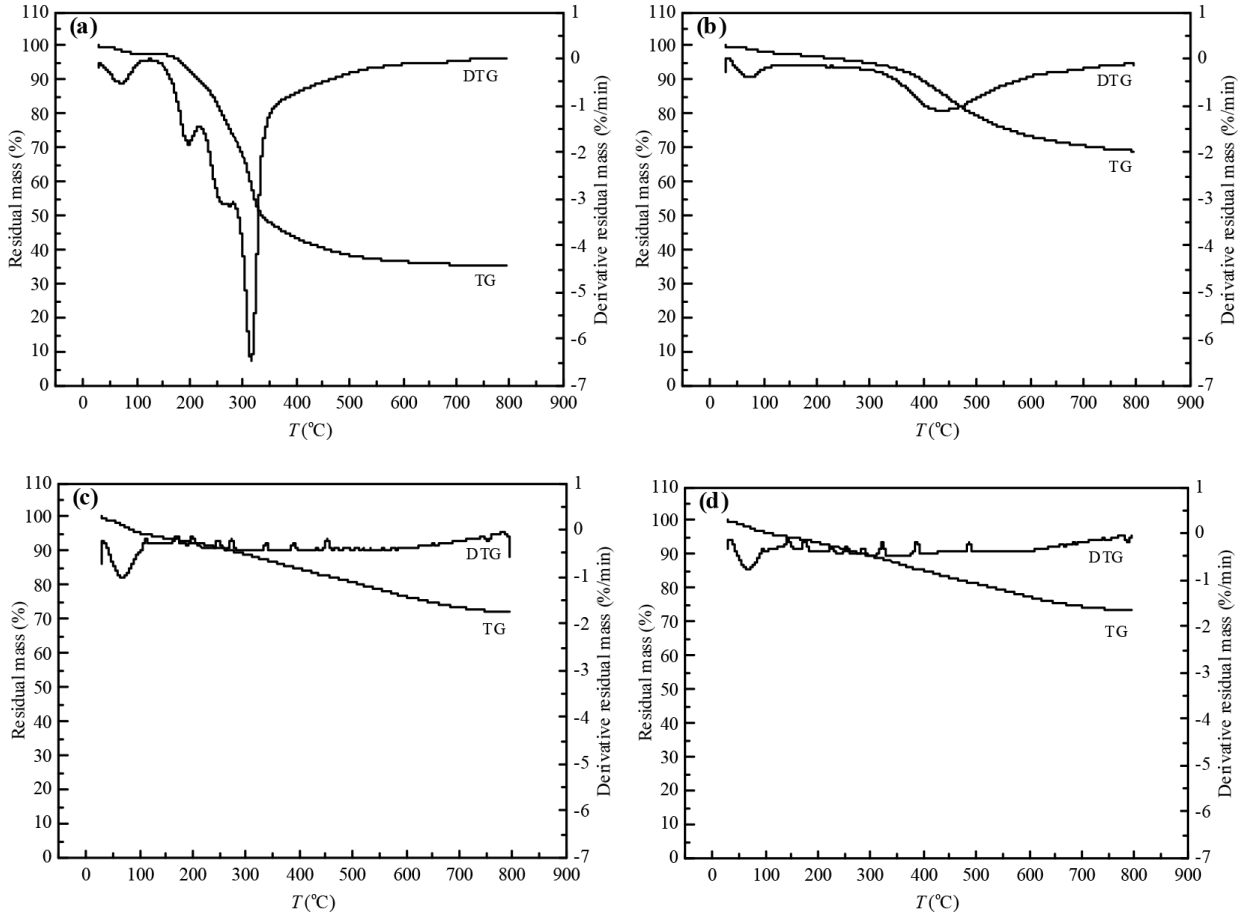

Fig. 4. TG-DTG of (a) raw coconut shell, (b) coconut shell after carbonization, (c) coconut shell activated carbon by chemical activation with KOH, and (d) coconut shell activated carbon after adsorption.

clearly demonstrate that the removal efficiency increases up to the optimum dosage beyond which the increase in removal efficiency is negligible.

3.3.3. Effect of pH value

The pH value of aqueous solution is a significant parameter in the adsorption process. The results are displayed in Fig. 5c. As shown in the figure, the maximum adsorption is found at pH = 6, and the corresponding percent removal of lysine is 84%. With the increase of pH value beyond 6, the percent removal decreases.

It can be explained as follows. Lysine has four ion forms in aqueous solution, which is lys^{2+}, lys^{+}, $lys^{\pm}$ and lys^{-} depending on the pH. The pH of the solution affects the dissociation pattern of lysine in solution. In the pH ranging from 1 to 6, lysine is mainly in the form of lys^{2+} and lys^{+} in the solution. The content of lys^{2+} in solution decreases with the increase of pH value, and disappeared at pH 5. While the content of lys^{+} in the solution increased with the increase of pH value, and the maximum is found at pH = 6–7. After pH above 7, $lys^{\pm}$ ions began to appear in the solution, while the content of lys^{+} decreased gradually. The curve of lys^{+} with pH was in agreement with that of coconut shell activated carbon adsorption, indicating that coconut shell activated carbon mainly adsorbed lys^{+} in aqueous solution. Thus, the pH value of 6 was selected for further studies.

3.3.4. Adsorption isotherm

With the aim of acquiring the capacity and thermodynamics of lysine adsorption on coconut shell activated carbon, adsorption isotherms were carried out at the temperature of 20, 30 and 40°C, respectively. Moreover, Langmuir and Freundlich isotherm models were used to establish the mechanism for lysine adsorption on the coconut shell activated carbon. The linear form of these models were listed as follows [46].

$$\frac{C_e}{q_e} = \frac{1}{q_m} C_e + \frac{1}{K_L q_m} \tag{4}$$

$$In\, q_e = \frac{1}{n} InC_e + InK_F \tag{5}$$

where q_m (mg/g) is the mono layer adsorption capacity of the adsorbent. K_L is the Langmuir adsorption constant. K_F and n are the Freundlich constants, where K_F and n represent the adsorption capacity and intensity of adsorption, respectively. The values of the Langmuir constants, Freun-

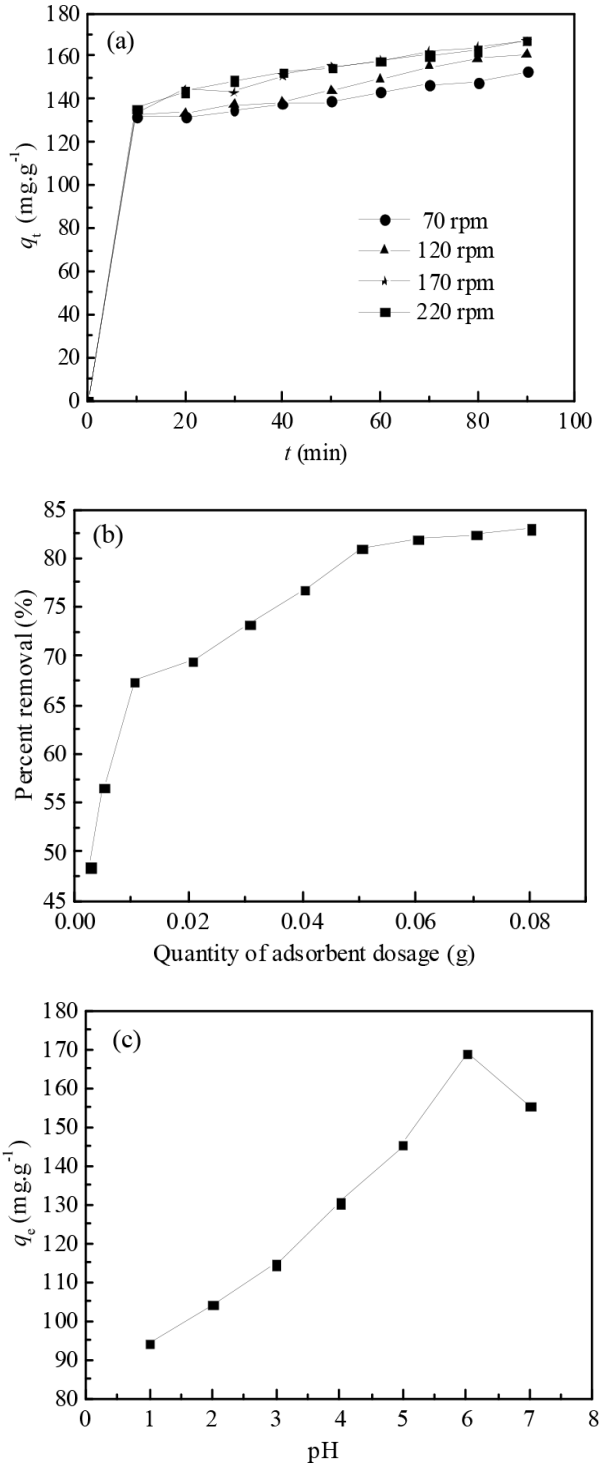

Fig. 5. Effect of (a) shaking speed, (b) adsorbent dosage, and (c) pH on the adsorption of lysine.

dlich constants, and the correlation coefficients were listed in Table 4, and the Langmuir and Freundlich adsorption isotherms are displayed in Figs. 6 and 7, respectively.

As shown in Table 4, the correlation coefficients, R^2, of Langmuir model for lysine are all more than 0.994, which are higher than of Freundlich model at the three different

Table 4
Langmuir and Freundlich isotherm constants for the adsorption of lysine

T(°C)	Langmuir model			Freundlich model		
	q_m (mg/g)	K_L (L/mg)	R^2	K_F (mg/g)	$1/n$	R^2
20	96.15	0.1186	0.9944	34.20	0.1782	0.7315
30	93.46	0.1202	0.9956	32.76	0.1828	0.7593
40	92.59	0.1756	0.9940	32.19	0.1848	0.7796

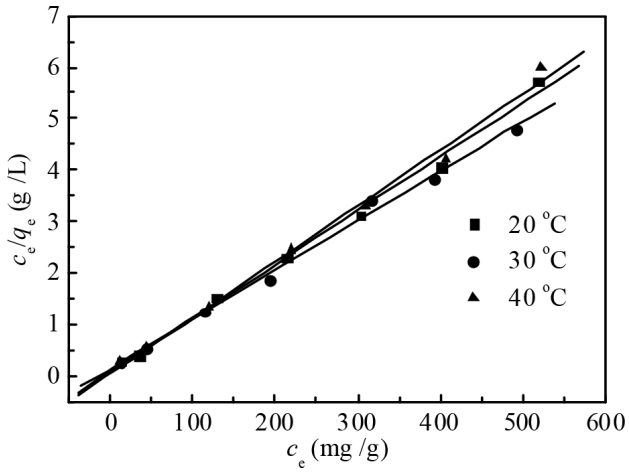

Fig. 6. Langmuir isotherm adsorption curve.

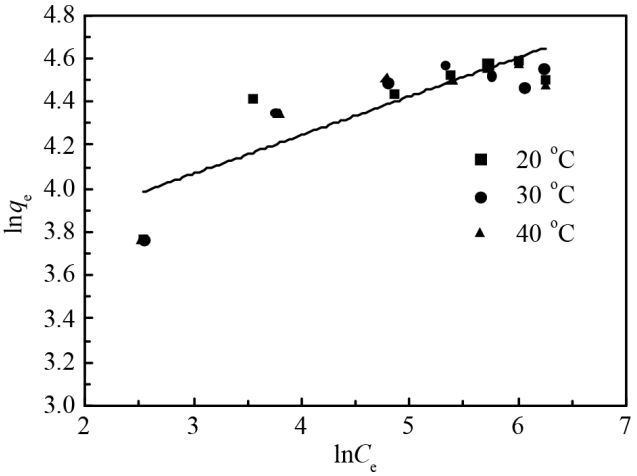

Fig. 7. Freundlich isotherm adsorption curve.

temperatures, respectively. Therefore, Langmuir model is more suitable for describing the adsorption equilibrium of lysine on the coconut shell activated carbon, and the mono layer surface adsorption occurs on the specific homogeneous sites, the similar results was found by Chen [10].

Furthermore, the thermodynamic parameters, such as enthalpy change ΔH, entropy change ΔS and Gibbs free energy change ΔG, was calculated using the following equations [47].

$$InK_L = \frac{\Delta H}{RT} + \frac{\Delta S}{R} \quad (6)$$

$$\Delta G = \Delta H - T\Delta S \quad (7)$$

The data of lnK_L versus $1/T$ were plotted and a linear relationship was found with the values of slope and intercept determined to be –1783.1 and 10.797. The thermodynamic values of ΔH, ΔS and ΔG were determined and are listed in Table 5. As shown in Table 5, the negative ΔG decrease slightly with the increasing of temperature, which indicate that the lysine adsorption on coconut shell activated carbon is spontaneous. The positive values of ΔS demonstrate that the lysine adsorption on coconut shell activated carbon is entropy driven rather than enthalpy driven [48]. Moreover, the positive value of ΔH confirms the endothermic nature of the lysine adsorption on coconut shell activated carbon and increasing temperature favors the adsorption.

3.3.5. Adsorption kinetics

The kinetic of the adsorption data were correlated using two different kinetic models: the pseudo first-order [Eq. (8)], and pseudo second-order [Eq. (9)] [49].

$$In\left(q_e - q_t\right) = Inq_e - k_1 t \quad (8)$$

where q_e and q_t (mg/g) are the amounts of adsorbate adsorbed at equilibrium and at any time, t (min), respectively. k_1 (min^{-1}) is the rate constant of pseudo first-order model. The plot of ln ($q_e - q_t$) versus t gave the slope of k_1 and intercept of lnq_e at different temperatures, as exhibited in Fig. 8. The values of k_1 and correlation coefficient R^2 obtained for the plots were listed in Table 6. The values of R^2 were relatively small, which varied from 0.6324 to 0.8829. It indicates that the pseudo first-order model is not suitable for describing the adsorption of lysine on the activated carbon.

$$\frac{t}{q_t} = \frac{1}{q_e}t + \frac{1}{k_2 q_e^2} \quad (9)$$

where k_2 (g/(mg·min)) is the rate constant of second-order kinetic model. The linear plot of t/q_t versus t gave 1/q_e as the slope and $1/k_2\, q_e^{\,2}$ as the intercept. The linear plot of t/q_t vs. t, as displayed in Fig. 9, exhibits a well agreement between the experimental and the correlated q_e values (Table 5). Furthermore, the correlation coefficient values for the second-order kinetic model were higher than 0.996, which indicates the applicability of the second-order kinetic model to describe the adsorption of lysine on the prepared activated carbon. However, Chen et al. [10] have found that the adsorption kinetics of lysine on spherical lignin beads can be well described by the pseudo first-order model.

Table 5
Thermodynamic parameters for the adsorption of lysine

T (°C)	ΔH (kJ/mol)	ΔS (J/mol·K)	ΔG (kJ/mol)
20.0			–28.5
30.0	2.71	107.2	–29.5
40.0			–31.4

The adsorption activation energy was calculated by the logarithmic form of Arrhenius equation as follows.

$$In\,K_2 = -\frac{E_a}{RT} + In\,A \quad (10)$$

where T is the absolute temperature (K), R is the gas constant (8.314 J/mol·K), E_a is the adsorption activation energy (kJ/mol), and A is frequency factor.

The data of lnk_2 versus $1/T$ were plotted and displayed a good linear relationship. The correlation coefficient R^2 is 0.9708. The fitted equation is as follows.

$$In\,K_2 = -\frac{3628.8}{T} - 18.24 \quad (11)$$

The adsorption activation energy (E_a), –30.2 kJ/mol, was calculated by the above equation. The negative adsorption energy may be explained by the combinations of many element chemical adsorption.

3.4. Desorption study

Desorption is a significant complement of adsorption to recover the lysine and reuse the activated carbon. An acidic pH was favorable for the adsorption of lysine on activated carbon, and the desorption of lysine can be achieved in alkaline environment. The results of desorption experiments are exhibited in Fig. 10. Along with the increasement of ammonia concentration from 0.25 mol/L to 1.50 mol/L, the desorption efficiency for lysine is rapidly increased from 51.6% to 93.8%, and then slowly rised to 95.8% from the ammonia concentration 1.50 mol/L to 2.50 mol/L. Meanwhile, the lysine adsorption efficiency of activated carbon remained almost constant for the four cycles of adsorption and desorption, which exhibit that there are no irreversible sites on the surface of the activated carbon. The lysine was recovered by the backwashing process with the ammonia solution which provides a valid method of recycling lysine.

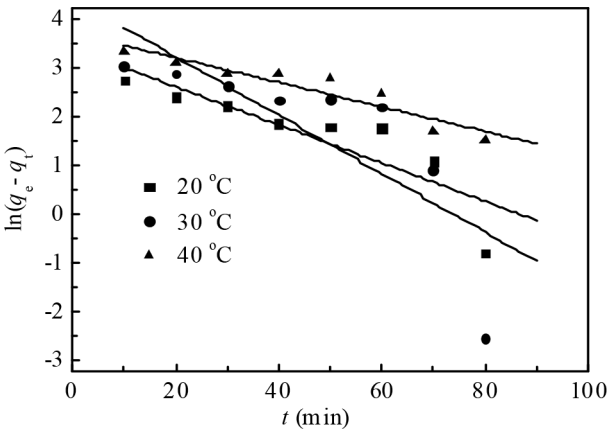

Fig. 8. Pseudo first-order kinetic model for adsorption of lysine on coconut shell activated carbon.

Table 6
Adsorption kinetics parameters

T (°C)	$q_{e,exp}$ (mg/g)	Pseudo-first-order kinetic model			Pseudo-second-order kinetic model		
		$q_{e,cal}$ (mg/g)	k_1 (min^{-1})	R^2	$q_{e,cal}$ (mg/g)	k_2 (g/mg·min)	R^2
20	141.31	29.93	0.0393	0.7541	143.68	2.96×103	0.9992
30	149.08	83.83	0.0601	0.6324	153.61	1.75×103	0.9977
40	158.65	41.07	0.0253	0.8829	162.60	1.34×103	0.9962

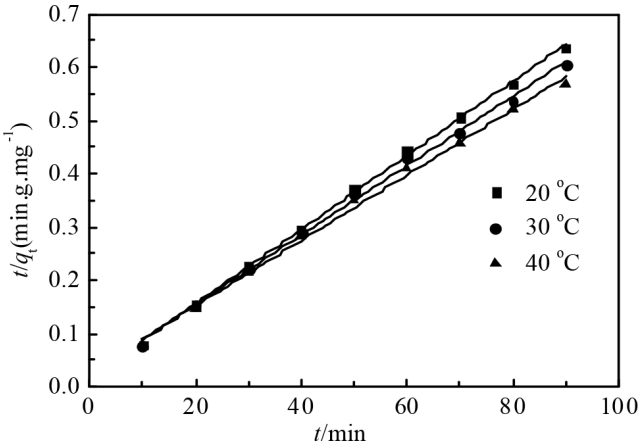

Fig. 9. Pseudo second-order kinetic model for adsorption of lysine on coconut shell activated carbon.

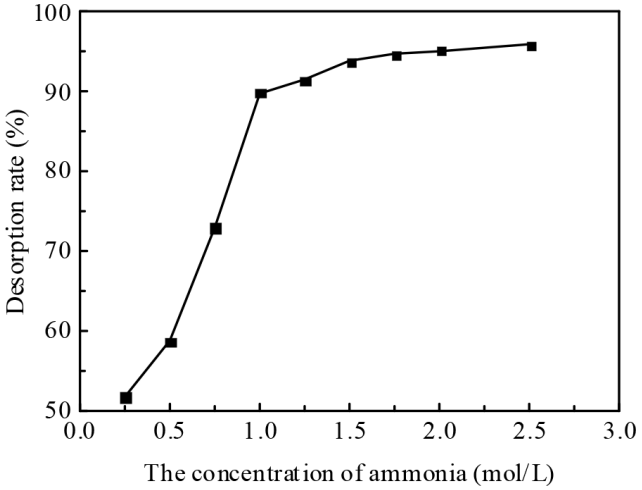

Fig. 10. Desorption of lysine loaded activated carbon by ammonia.

4. Conclusions

(1) The activated carbon was synthesized from coconut shell by chemical activation with potassium hydroxide. Through the orthogonal experiment, the optimum condition is that carbonized material/KOH ratio of 2.0, activation time of 1.5 h, carbonization temperature of 600°C and activation temperature of 350°C, respectively.

(2) SEM images and BET data indicate that coconut shell activated carbon is an effective adsorbent which has the maximum surface area and pore volume compare to the raw coconut shell and carbonized material.

(3) In the batch experiments, the effect of external diffusion is negligible at 170 rpm, the percent removal of lysine increases with the increment of the adsorbent dosage, the optimum pH is 6. The adsorption equilibrium data of lysine on coconut shell activated carbon agree well with the Langmuir model. The adsorption process is of the monolayer variety and it is a favorable adsorption. The adsorption process is well described by the pseudo second-order equation.

(4) The desorption using the solution of ammonia is suitable for desorption and reusing process. The results indicates that activated carbon could be employed as a promising and effective adsorbent for the removal of lysine from aqueous solutions.

Acknowledgements

We acknowledge the financial support for this work from the Fujian Provincial Collaborative Innovation Center for Clean Coal Gasification Technology (XK1705), the Educational Research Project of Young and Middle-aged Teacher of Fujian Province (JT180625 and JAT170852), and the Distinguished Young Researcher Training Project in Universities of Fujian Province (Project No. Fujian Education Science [2017]52).

References

[1] N. Kitadai, T. Yokoyama, S. Nakashima, ATR-IR spectroscopic study of L-lysine adsorption on amorphous silica, J. Colloid Interf. Sci., 329(1) (2009) 31–37.
[2] C. Cherkouk, L. Rebohle, W. Skorupa, Lysine adsorption on the silanized SiO_2-surface for immobilization of the estrogen receptor hERα, Appl. Surf. Sci., 257(11) (2011) 4831–4835.
[3] P.J. Reeds, Dispensable and indispensable amino acids for humans, J. Nutr., 130(7) (2000) 1835–1840.
[4] Z. Lou, Q. Zeng, X. Chu, F. Yang, D. He, M. Yang, H. Fan, First-principles study of the adsorption of lysine on hydroxyapatite (100) surface, Appl. Surf. Sci., 258(11) (2012) 4911–4916.
[5] N. Kitadai, T. Yokoyama, S. Nakashima, In situ ATR-IR investigation of L-lysine adsorption on montmorillonite, J. Colloid Interf. Sci., 338(2) (2009) 395–401.
[6] N.M. Torbatinejad, S.M. Rutherfurd, P.J. Moughan, Total and reactive lysine contents in selected cereal-based food products, J. Agr. Food Chem., 53(11) (2005) 4454–4458.

[7] P.J. Moughan, S.M. Rutherfurd, Available lysine in foods: a brief historical overview, J. AOAC Int., 91(4) (2008) 901–906.
[8] M. Kircher, W. Pfefferle, The fermentative production of L-lysine as an animal feed additive, Chemosphere, 43(1) (2001) 27–31.
[9] T. Tateno, H. Fukuda, A. Kondo, Production of L-Lysine from starch by Corynebacterium glutamicum displaying α-amylase on its cell surface, Appl. Microbiol. Biot., 74(6) (2007) 1213–1220.
[10] G. Chen, M. Liu, Adsorption of L-lysine from aqueous solution by spherical lignin beads: Kinetics and equilibrium studies, Bioresour., 7(1) (2011) 0298–0314.
[11] J. Rodríguez-Martínez, S.Y. Martínez-Amador, Y. Garza-García, Comparative anaerobic treatment of wastewater from pharmaceutical, brewery, paper and amino acid producing industries, J. Ind. Microbiol. Biot., 32(11–12) (2005) 691–696.
[12] T.V. Elisseeva, V.A. Shaposhnik, I.G. Luschik, Demineralization and separation of amino acids by electro dialysis with ion-exchange membranes, Desalination, 149(1) (2002) 405–409.
[13] F. Yuan, Q. Wang, P. Yang, Y. Tian, W. Cong, Influence of different resins on the amino acid recovery by resin-filling electro dialysis, Sep. Purif. Technol., 153 (2015) 51–59.
[14] R. Widyarani, N.A. Bowden, R.C. Kolfschoten, J.P. Sanders, M.E. Bruins, Fractional precipitation of amino acids from agro-industrial residues using ethanol, Ind. Eng. Chem. Res., 55(27) (2016) 7462–7472.
[15] S. Tsukahara, B. Nanzai, M. Igawa, Selective transport of amino acids across a double membrane system composed of a cation-and an anion-exchange membrane, J. Membr. Sci., 448 (2013) 300–307.
[16] J.J. Keating, S. Bhattacharya, G. Belfort, Separation of D, L-Amino acids using ligand exchange membranes, J. Membr. Sci., 555 (2018) 30–37.
[17] J. Wei, Adsorption and cracking of n-alkanes over ZSM-5: negative activation energy of reaction, Chem. Eng. Sci., 51(11) (1996) 2995–2999.
[18] A. Parbhakar, J. Cuadros, M.A. Sephton, W. Dubbin, B.J. Coles, D. Weiss, Adsorption of L-lysine on montmorillonite, Colloid. Surface A., 307(1–3) (2007) 142–149.
[19] B. Heibati, S. Rodriguez-Couto, A. Amrane, M. Rafatullah, A. Hawari, M.A. Al-Ghouti, Uptake of reactive black 5 by pumice and walnut activated carbon: chemistry and adsorption mechanisms, J. Ind. Eng. Chem., 20(5) (2014) 2939–2947.
[20] A.J. O'Connor, A. Hokura, J.M. Kisler, S. Shimazu, G.W. Stevens, Y. Komatsu, Amino acids adsorption onto mesoporous silica molecular sieves, Sep. Purif. Technol., 48(2) (2006) 197–201.
[21] J. Goscianska, A. Olejnik, R. Pietrzak, Adsorption of L-phenylalanine onto mesoporous silica, Mater. Chem. Phys., 142 (2013) 586–593.
[22] M. Hadri, Z. Chaouki, K. Draoui, M. Nawdali, A. Barhoun, H. Valdes, N. Drouichee, H. Zaitana, Adsorption of a cationic dye from aqueous solution using low-cost Moroccan diatomite: adsorption equilibrium, kinetic and thermodynamic studies, Desal. Water Treat., 75 (2017) 213–224.
[23] C. Djelloula, A. Hasseineb, O. Hamdaouic, Adsorption of cationic dye from aqueous solution by milk thistle seeds: isotherm, kinetic and thermodynamic studies, Desal. Water Treat., 78 (2017) 313–320.
[24] M. Liu, J. Huang, Y. Deng, Adsorption behaviors of L-arginine from aqueous solutions on a spherical cellulose adsorbent containing the sulfonic group, Bioresour. Technol., 98 (2007) 1144–1148.
[25] L. Cermakova, I. Kopecka, M. Pivokonsky, L. Pivokonska, V. Janda, Removal of cyanobacterial amino acids in water treatment by activated carbon adsorption, Sep. Purif. Technol., 173 (2017) 330–338.
[26] M. Rafatullah, T. Ahmad, A. Ghazali, O. Sulaiman, M. Danish, R. Hashim, Oil palm biomass as a precursor of activated carbons: a review, Crit. Rev. Environ. Sci. Technol., 43(11) (2013) 1117–1161.
[27] T. Ahmad, M. Danish, M. Rafatullah, A. Ghazali, O. Sulaiman, R. Hashim, M.N.M. Ibrahim, The use of date palm as a potential adsorbent for wastewater treatment: a review, Environ. Sci. Pollut. Res., 19(5) (2012) 1464–1484.
[28] M. Goswami, P. Phukan, Enhanced adsorption of cationic dyes using sulfonic acid modified activated carbon, J. Environ. Chem. Eng., 5(4) (2017) 3508–3517.
[29] M. Daoud, O. Benturki, Z. Kecira, P. Girods, A. Donnot, Removal of reactive dye (BEZAKTIV Red S-MAX) from aqueous solution by adsorption onto activated carbons prepared from date palm rachis and jujube stones, J. Mol. Liq., 243 (2017) 799–809.
[30] K. Björklund, L.Y. Li, Adsorption of organic storm water pollutants onto activated carbon from sewage sludge, J. Environ. Manage., 197 (2017) 490–497.
[31] B. Zhang, X. Han, P. Gu, S. Fang, J. Bai, Response surface methodology approach for optimization of ciprofloxacin adsorption using activated carbon derived from the residue of desilicated rice husk, J. Mol. Liq., 238 (2017) 316–325.
[32] B. Köse, S. Erentürk, Removal of Pb (II) from water by carbonized walnut shell: characterization of adsorbent, adsorption capacity, kinetic, thermodynamic and isotherm studies, Desal. Water Treat., 60 (2017) 301–309.
[33] A.A. Olajire, J.J. Abidemi, A. Lateef, N.U. Benson, Adsorptive desulphurization of model oil by Ag nano particles-modified activated carbon prepared from brewer's spent grains, J. Environ. Chem. Eng., 5(1) (2017) 147–159.
[34] H. Demiral, C. Güngör, Adsorption of copper (II) from aqueous solutions on activated carbon prepared from grape bagasse, J. Clean. Prod., 124 (2016) 103–113.
[35] J.V. Flores-Cano, M. Sánchez-Polo, J. Messoud, I. Velo-Gala, R. Ocampo-Pérez, J. Rivera-Utrilla, Overall adsorption rate of metronidazole, dimetridazole and diatrizoate on activated carbons prepared from coffee residues and almond shells, J. Environ. Manage., 169 (2006) 116–125.
[36] M. Kobya, Adsorption, kinetic and equilibrium studies of Cr (VI) by hazelnut shell activated carbon, Adsorption Sci. Technol., 22(1) (2004) 51–64.
[37] M. Kumar, R. Tamilarasan, Modeling studies for the removal of methylene blue from aqueous solution using Acacia fumosa seed shell activated carbon, J. Environ. Chem. Eng., 1(4) (2013) 1108–1116.
[38] S. Babel, T.A. Kurniawan, Cr (VI) removal from synthetic wastewater using coconut shell charcoal and commercial activated carbon modified with oxidizing agents and/or chitosan, Chemosphere, 54(7) (2004) 951–967.
[39] N. Singh, C. Balomajumder, Simultaneous removal of phenol and cyanide from aqueous solution by adsorption onto surface modified activated carbon prepared from coconut shell, J. Water Process Eng., 9 (2016) 233–245.
[40] L. Yue, Q. Xia, L. Wang, L. Wang, H. DaCosta, J. Yang, X. Hu, CO_2 adsorption at nitrogen-doped carbons prepared by K_2CO_3 activation of urea-modified coconut shell, J. Colloid Interf. Sci., 511 (2018) 259–267.
[41] A.T. Mohd Din, B.H. Hameed, A.L. Ahmad, Batch adsorption of phenol onto physiochemical- activated coconut shell, J. Hazard. Mater., 161(2–3) (2009) 1522.
[42] G. Jiang, L. Wen, F. Chen, F. Wu, S. Lin, B. Yang, Structural characteristics and antioxidant activities of polysaccharides from longan seed, Carbohyd. Polym., 92(1) (2013) 758–764.
[43] M.A. Olutoye, B.H. Hameed, Production of biodiesel fuel by transesterification of different vegetable oils with methanol using Al_2O_3 modified MgZnO catalyst, Bioresour. Technol., 132 (2013) 103–108.
[44] J. Acharya, J.N. Sahu, B.K. Sahoo, C.R. Mohanty, B.C. Meikap, Removal of chromium (VI) from wastewater by activated carbon developed from Tamarind wood activated with zinc chloride, Chem. Eng. J., 150(1) (2009) 25–39.
[45] W. Li, K. Yang, J. Peng, L. Zhang, S. Guo, H. Xia, Effects of carbonization temperatures on characteristics of porosity in coconut shell chars and activated carbons derived from carbonized coconut shell chars, Ind. Crop. Prod., 28(2) (2008) 190–198.

[46] L. Wang, W. Liu, T. Wang, J. Ni, Highly efficient adsorption of Cr(VI) from aqueous solutions by amino-functionalized titanate nano tubes, Chem. Eng. J., 225 (2013) 153–163.
[47] A.M. Aljeboree, A.N. Alshirifi, A.F. Alkaim, Kinetics and equilibrium study for the adsorption of textile dyes on coconut shell activated carbon, Arabian J. Chem., 10 (2017) S3381–S3393.
[48] S. Banerjee, Y.C. Sharma, Equilibrium and kinetic studies for removal of malachite green from aqueous solution by a low cost activated carbon, J. Ind. Eng. Chem., 19(4) (2013) 1099–1105.
[49] J. Yang, M. Yu, W. Chen, Adsorption of hexavalent chromium from aqueous solution by activated carbon prepared from longan seed: Kinetics, equilibrium and thermodynamics, J. Ind. Eng. Chem., 21 (2015) 414–422.